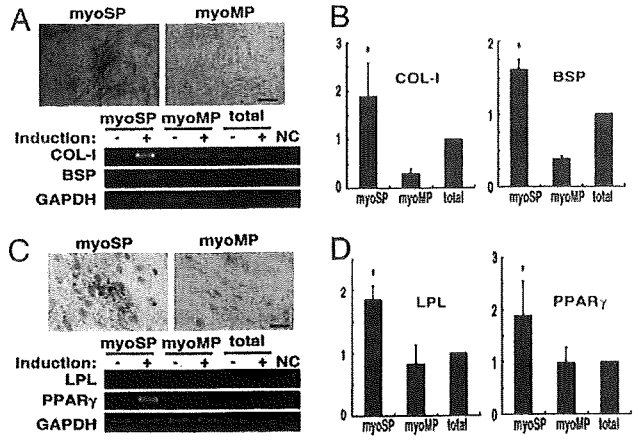

Fig. 5. Multidifferentiation capacity of myoSP. (*A*). Induction of osteocyte differentiation of myoSP, but not myoMP, as determined by alkaline phosphatase staining (*Upper*) and by RT-PCR for the expression of osteoblast lineage-specific genes (*Lower*). (Scale bar, 500 m.) (*B*) Relative mRNA expression of the indicated osteocyte markers in myoSP, myoMP, and whole myometrial tissues was examined by semiquantitative RT-PCR and normalized for GAPDH expression. Each bar indicates the mean SEM of the relative expression ratio obtained from three independent experiments using three individual samples. *, *P* 0.05, versus myoMP. (*C*) Induction of adipocyte differentiation of myoSP, but not myoMP, as determined by Oil red-O staining (*Upper*) and by RT-PCR for the expression of adipocyte lineage-specific genes (*Lower*). (Scale bar, 250 m.) (*D*) Each bar indicates the mean SEM of the relative mRNA expression of the adipocyte markers from three independent experiments using three individual samples. *, *P* 0.05, versus myoMP. Induction ( ) and ( ) indicate the 21-day treatment with control media and osteocyte- (*C*) or adipocyte- (*D*) inducing media, respectively.

We found that human-derived cells (Vm-positive) expressing SMA were present only in the uteri of the NOG mice transplanted with myoSP (Fig. 4*A Upper*), but not myoMP (data not shown), which was similar to the results of the nonpregnant E_2-treated uteri (Fig. 3). Immunofluorescence staining and confocal microscopic analysis of the serial cryosections revealed that the human myometrial cells doubly positive for SMA and Vm in the pregnant uteri contained a larger number of OTR-positive cells (Fig. 4*A Lower* and SI Fig. 8) than those present in the nonpregnant E_2-treated uteri (Fig. 4*B*). In agreement with a previous report (21), endometrial glands were positive for OTR (Fig. 4*B*). Thus, undifferentiated myoSP had not only the potentials of proliferating and differentiating into the mature myometrial cells in the mouse uteri but also the capacity of inducing the expression of OTR particularly in the pregnant uteri.

Lastly, we examined the potential of myoSP for multilineage differentiation. We cultured and expanded myoSP and myoMP under hypoxic condition for 2–4 weeks and then replaced the media with "osteogenesis-inducing medium" for induction of osteogenesis or "adipogenic induction and maintenance medium" for adipogenesis, and further cultured under normoxic condition for another 2 weeks. In the presence of osteogenesis-inducing medium, myoSP, but neither myoMP nor unfractionated myometrial cells, exhibited an apparent alkaline phosphatase activity together with significant up-regulation of collagen type 1 (COL-I), bone sialoprotein (BSP), and several other osteogenesis marker genes (Figs. 5 *A* and *B* and SI Fig. 9). Similarly, treatment with adipogenic induction and maintenance medium for 2 weeks induced adipogenesis in myoSP, but neither myoMP nor unseparated myometrial cells, as judged by enlarged and rounded morphology, staining with a lipid dye Oil red O, and significant up-regulation of lipoprotein lipase (LPL) and peroxisome-proliferating activated receptor (PPAR) genes, both adipose-specific markers (Figs. 5 *C* and *D*).

Discussion

The results of this study are a strong argument in support of myometrial stem cells. These cells retain the capability to differentiate into multiple cell types as well as smooth muscle cells *in vitro* and to give rise to myometrial tissues *in vivo*. We isolated these stem-like or progenitor cells, the myoSP population, from human myometrium and found that they survived and proliferated *in vitro* only under hypoxic conditions. There is an enlarging body of evidence supporting that low-oxygen conditions enhance the proliferation of adult stem cells and that proliferation in a hypoxic environment is one characteristic that defines the stem cell (14, 15). Thus, the requirement of a hypoxic environment for the survival and expansion of myoSP further substantiates that they are bona fide tissue-specific stem cells.

The requirement of a hypoxic environment for myoSP culture and spontaneous differentiation into smooth muscle cells may implicate myoSP in the pathogenesis of myometrium-derived neoplasms, notably leiomyomas. Leiomyomas are the most common gynecological tumors in women of reproductive age and are associated with a variety of symptoms including abnormal uterine bleeding, pelvic pain, urinary frequency, impaired fertility, and spontaneous abortion. They are clonal in origin (22), and their development is thought to be induced and promoted by hypoxia (23–25). Low oxygen tension (1–5% O_2) dramatically up-regulates secreted frizzled-related protein 1, a modulator of Wnt signaling, which exerts antiapoptotic effects in leiomyoma cells but not myometrial cells (25). Myometrial contractions and vasoconstriction that occur during menstruation render the myometrium hypoxic. It is possible that repeated menstruation-induced hypoxia may select a single cell such as a myoSP to proliferate and acquire cytogenetic abnormalities that would ultimately result in the development of a leiomyoma. Leiomyomas occasionally contain adipogenic components and are referred to as lipoleiomyomas (26) and, very rarely, they become ossified (27), which is consistent with the potential of myoSP for differentiation not only into myocytes but also into adipocytes and osteocytes. In support of our idea, Arango *et al.* (28) have reported that Müllerian duct mesenchyme-specific disruption of -catenin results in a progressive turnover of uterine myometrium to adipose tissue, suggesting a possible existence of myometrial stem/progenitor cells that have the potential for differentiating into adipocytes in the absence of -catenin and eventually giving rise to lipoleiomyomas. Indeed, the same group has recently isolated a myometrial SP from the mouse uterus and provided evidence suggesting that the SP contains putative myometrial stem/progenitor cells derived from the Müllerian duct mesenchyme (29), which supports the enrichment of stem/progenitor cells in myoSP in humans.

Human subendometrial myometrium originates from the Müllerian duct, whereas the outer myometrium has non-Müllerian origin (30); however, they both are derived from the mesenchyme (31). In addition to the origin of the myometrium, the present results demonstrating the quiescent and undifferentiated status of myoSP, its multidifferentiation potential, and self-renewal/reconstitution capability suggest that myoSP may share many characteristics of so-called mesenchymal stem cells (MSCs). MSCs are defined as self-renewable, multipotent progenitor cells with the capacity to differentiate into several distinct mesenchymal lineages (32). However, there exist some phenotypic and functional differences. First, although myoSP expressed several MSC markers including CD90, CD73, CD105, and STRO-1 (SI Fig. 6*B*), the majority of myoSP was CD34-positive and CD44-negative (Fig. 1*B* and SI Fig. 6*B*), whereas MSCs are known to be negative for CD34 and positive for CD44 (33). Second, myoMP also expressed STRO-1 like MSCs; however, it did not possess stem cell-like properties. Third, unlike bone marrow- or peripheral blood-derived MSCs (32), myoSP

did not generate skeletal muscle cells when we transplanted them into the intact or chemically injured skeletal muscle of NOG mice (SI Fig. 10). Further studies will be required to elucidate a mechanism by which myoSP behaves in a different way from MSCs in response to the microenvironment and/or niche of various tissues and organs.

We here demonstrated that myoSP, whose ESR1 expression level was relatively low, generated myometrial tissues efficiently under the influence of E_2. It is conceivable that mouse myometrial ESR-1-positive cells may produce and secret bioactive substances in response to estrogen, which, in turn, may drive transplanted myoSP to proliferate and differentiate into mature myometrial cells in a paracrine manner. In this regard, there may similar mechanism(s) underlying the contribution of myoSP to the hormone-induced remodeling and expansion of human uterus. In support of this idea, Chan *et al.* (34) have reported that label-retaining cells, which are thought to correspond to quiescent tissue-specific stem cells, are negative for ESR1 in the endometrial epithelium but ESR1-positive in the stroma, suggesting the capacity of the stromal stem/progenitor cells to respond to estrogen and transmit paracrine signals to epithelial cells for endometrial epithelium regeneration. Besides myometrial cell growth, E_2 and ESR1 are also involved in the induction of OTR (35), one of the acquired functional properties of myometrium throughout pregnancy, in particular, during the late pregnancy and labor (18–20). In this study, human OTR was dramatically up-regulated in the pregnant uterus compared with nonpregnant E_2-treated uterus. These facts collectively raise a possibility that, in addition to E_2, certain cell growth-promoting microenvironmental factors of mouse pregnant uterus may contribute to the induction of human OTR in the regenerated human myometrium, and that there may be some similarities in those factors between mouse and human.

A thorough characterization of myoSP is a prerequisite for understanding the complex mechanisms underlying the morphogenesis and physiological regeneration of the myometrium. Our procedures for isolating and cultivating myoSP have made these studies possible. The elucidation of functions and cellular properties of myoSP will broaden our understanding of pathogenesis of myometrium-derived diseases notably leiomyomas. Additionally, the techniques developed by our laboratory for culturing and differentiating myoSP could be a starting point for using these cells for the regeneration of the uterus or other organs.

Materials and Methods

Detailed protocols can be found in *SI Methods*.

Preparation of Human Myometrial Cells. Normal myometrial tissues without any abnormalities including adenomyosis or malignancies were obtained from 63 women (age range 35–54 years) undergoing hysterectomy for benign gynecological diseases. The use of these human specimens was approved by the Keio University Ethics Committee, and all patients provided informed consent. The myometrial tissue was cut up manually into small pieces of 1 mm^3 which were then incubated for 4–16 h in Dulbecco's modified Eagle's medium (Sigma–Aldrich) containing 0.2% (wt/vol) collagenase (Wako), 0.05% DNase I (Invitrogen), 1% antibiotic-antimycotic mixture (Invitrogen), 10% FBS and 10 mM Hepes buffer solution (Invitrogen) at 37°C on a shaker. After the shaking, the digested tissue was filtered through a sterile 400- m polyethylene mesh filter to remove undigested tissues, and again filtered through a 40- m cell strainer (BD–Falcon). The filtrates were layered over Ficoll-Paque PLUS (Amersham Biosciences) and centrifuged to remove red blood cells. The media/Ficoll interface layer was aspirated, washed, and disaggregated in a 0.05% trypsin-EDTA solution (Sigma–Aldrich) containing 0.05% DNase I by pipetting to obtain single-cell suspensions.

Hoechst 33342 and Pyronin Y (PY) Staining. The dissociated myometrial cells were resuspended at a concentration of 2 10^6 cells per milliliter in SP solution (calcium- and magnesium-free Hanks' balanced salt solution containing 2% FBS, 1% penicillin/streptomycin, and 10 mM Hepes). Hoechst 33342 (Sigma–Aldrich) was then added at a final concentration of 5 g/ml and the sample incubated at 37°C for 90 min. A parallel aliquot was stained with Hoechst dye in the presence of 50 M reserpine (Sigma–Aldrich). After incubation, the cells were centrifuged at 1,500 *g* for 7 min, resuspended in 2 ml of cold SP solution and further incubated with 1 g/ml propidium iodide (PI; Sigma–Aldrich) to label nonviable cells. The cells were kept on ice at all times after staining with the Hoechst 33342 dye. The Hoechst dye- and PI-treated cells were subjected to flow cytometric analysis to separate the myoSP and myoMP. For costaining with Hoechst 33342 and PY, sorted myoSP and myoMP were washed twice in SP solution, incubated with 1 g/ml Hoechst33342 together with 50 M reserpine in a 37°C water bath for 45 min, and then, without any additional washing, incubated with 3.3 M PY (Polysciences) for another 45 min. The cells were washed once in an excess volume of SP solution and subjected to FACS analysis. Cells cotreated with Hoechst and reserpine or treated with PY alone were used as negative controls. PY was excited with an argon laser.

Antibody Staining for FACS Analysis. Hoechst-stained single myometrial cells were resuspended in SP solution at 1–5 10^7 cells per milliliter. The antibodies used for FACS were conjugated with fluorescein isothiocyanate (FITC), phycoerythrin (PE), or allophycocyanin (APC) (SI Table 1). All incubations with antibodies were carried out on ice for 30 min. After antibody staining, the cells were washed with an excess amount of SP solution and resuspended in SP solution at a concentration of 1 10^7 cells per milliliter before FACS analysis.

FACS Analysis. Myometrial cells were sorted by a FACS Vantage SE flow cytometer (BD Biosciences) and analyzed with CellQuest software (BD Biosciences). After collecting 5 10^4 events, the SP and MP populations were defined as reported previously (4, 9) (for details see *SI Methods*).

RT-PCR. The primers used for PCR amplification are as listed in SI Table 2. Total RNA was extracted by using TRIzol Reagent (Invitrogen) and reverse transcribed with SuperScript III reverse transcriptase (Invitrogen) and random hexamers, according to the manufacturers' instructions. cDNA was synthesized from 60,000 to 200,000 myoSP or myoMP. An aliquot was then assayed for the relative amount of GAPDH signal. These data were then used to calculate a dilution factor for each sample, so that each contained the same concentration of GAPDH cDNA.

Cell Culture. Both myoSP and myoMP were cultured in MSC growth medium (MSCGM; Cambrex Bio Science) under normoxic (20% O_2) or hypoxic (2% O_2) conditions for 4 weeks. Cell proliferation activities were measured by using the Cell Titer 96 Aqueous One Solution Cell Proliferation Assay (Promega) according to the manufacturer's instructions.

For induction of differentiation, myoSP and myoMP were plated at a density of 5 10^3 cells per well in 96-well dishes with MSCGM and grown in a hypoxic environment until the cells reached confluence (14–28 days). Subsequently, the cultures were exported to a normoxic environment, fed with osteocyte differentiation media or adipogenic induction/maintenance media (Cambrex Bio Science) for 2 to 3 weeks, and then harvested for RNA extraction, or subjected to alkaline phosphatase staining or Oil red O staining (for details see *SI Methods*).

Transplantation Analysis. All experiments using NOG mice (Central Institute for Experimental Animals) were conducted in

accord with the Guide for the Care and Use of Laboratory Animals of the Keio University School of Medicine. At transplantation, both recipient ovaries were removed to eliminate the influence of endogenous estrogen and the animals s.c. implanted with single E_2 pellet (1.5 mg E_2 per pellet, Innovative Research of America). We have previously reported that the serum E_2 level in mice implanted with single E_2 pellet was 216 144 pg/ml (mean SE, n 3) (17). myoSP (5 10^4 cells) were injected into each uterine horn of 16 NOG mice by using a 29-gauge needle. The myoMP were similarly transplanted into 16 age-matched NOG mice. The uteri were excised 10 weeks after transplantation. Alternatively, NOG mice were mated to ICR males 2 weeks after myoSP or myoMP (5 10^4 cells) were injected into the uterine horn of each NOG mouse. The pregnant uteri were excised at 7.5 d.p.c.

Immunofluorescence and Confocal Microscopy. Immunofluorescence analyses were performed on cytospun myoSP and myoMP or cryosections derived from uteri transplanted with myoSP or myoMP. Glass slides onto which the cytospun cells were overlaid or sections were mounted were fixed with 4% PFA for 20 min and washed with PBS, followed by permeablization with 0.2% Triton X-100 in PBS for 10 min. After blocking with 10% FBS for 60 min, slides were successively stained with various antibodies as listed in SI Table 1, followed by incubation with secondary antibodies conjugated with Alexa Fluor 488 (Molecular Probes) or red fluorescent dye Cy3 (Sigma–Aldrich) to visualize the primary antibodies. Nuclei were stained by using Bisbenzimide H33258 (Sigma–Aldrich) or TOTO3 (Molecular Probes). Images were collected by using an inverted Leica DMIRE2 fluorescent microscope (Leica Microsystems) equipped with a CCD camera (VB-700; Keyence) and a Leica TCS SP2 confocal microscopy system. Some acquired images were subjected to three-dimensional reconstruction using LCS software (Leica).

Statistical Analysis. A P value was calculated by using the unpaired Student t test.

We thank Shouka Kan and the other gynecologists of Keiyu Hospital (Yokohama, Japan) for collection of human myometrial samples and Norikazu Tamaoki, Takayuki Ohkawa, Sadafumi Suzuki, and the members of T.M.'s, Y.M.'s, and H.O.'s laboratories for their experimental support. This study was supported, in part, by Grants-in-Aid from the Japan Society for the Promotion of Science (to T.M., Y.Y., and M.O.), by a National Grant-in-Aid for the Establishment of High-Tech Research Center in a Private University (to T.M.), and by a Grant-in-Aid from the 21st Century Centers of Excellence program of the Ministry of Education, Science, and Culture of Japan at Keio University.

1. Ramsey EM (1994) in *Anatomy of the Human Uterus* (Cambridge Univ Press, Cambridge, UK), pp 18–40.
2. Shynlova O, Oldenhof A, Dorogin A, Xu Q, Mu J, Nashman N, Lye SJ (2006) *Biol Reprod* 74:839–849.
3. Körbling M, Estrov Z (2003) *N Engl J Med* 349:570–582.
4. Goodell MA, Brose K, Paradis G, Conner AS, Mulligan RC (1996) *J Exp Med* 183:1797–1806.
5. Challen GA, Little MH (2006) *Stem Cells* 24:3–12.
6. Redvers RP, Li A, Kaur P (2006) *Proc Natl Acad Sci USA* 103:13168–13173.
7. Schienda J, Engleka KA, Jun S, Hansen MS, Epstein JA, Tabin CJ, Kunkel LM, Kardon G (2006) *Proc Natl Acad Sci USA* 103:945–950.
8. Montanaro F, Liadaki K, Volinski J, Flint A, Kunkel LM (2003) *Proc Natl Acad Sci USA* 100:9336–9341.
9. Matsuzaki Y, Kinjo K, Mulligan RC, Okano H (2004) *Immunity* 20:87–93.
10. Sakaguchi H, Fujimoto J, Aoki I, Tamaya T (2003) *Steroids* 68:11–19.
11. Quesenberry PJ, Colvin GA, Lambert JF (2002) *Blood* 100:4266–4271.
12. Young HE (2004) *Curr Top Microbiol Immunol* 280:71–109.
13. Arai F, Hirao A, Ohmura M, Sato H, Matsuoka S, Takubo K, Ito K, Koh GY, Suda T (2004) *Cell* 118:149–161.
14. Zhu LL, Wu LY, Yew DT, Fan M (2005) *Mol Neurobiol* 31:231–242.
15. Grayson WL, Zhao F, Izadpanah R, Bunnell B, Ma T (2006) *J Cell Physiol* 207:331–339.
16. Ito M, Hiramatsu H, Kobayashi K, Suzue K, Kawahata M, Hioki K, Ueyama Y, Koyanagi Y, Sugamura K, Tsuji K, *et al.* (2002) *Blood* 100:3175–3182.
17. Masuda H, Maruyama T, Hiratsu E, Yamane J, Iwanami A, Nagashima T, Ono M, Miyoshi H, Okano HJ, Ito M, *et al.* (2007) *Proc Natl Acad Sci USA* 104:1925–1930.
18. Kimura T, Takemura M, Nomura S, Nobunaga T, Kubota Y, Inoue T, Hashimoto K, Kumazawa I, Ito Y, Ohashi K, *et al.* (1996) *Endocrinology* 137:780–785.
19. Kubota Y, Kimura T, Hashimoto K, Tokugawa y, Nobunaga K, Azuma C, Saji F, Murata Y (1966) *Mol Cell Endocrinol* 124:25–32.
20. Siebel AL, Gehring HM, Reytomas IG, Parry LJ (2003) *Endocrinology* 144:4272–4275.
21. Takemura M, Nomura S, Kimura T, Inoue T, Onoue H, Azuma C, Saji F, Kitamura Y, Tanizawa O (1993) *Endocrinology* 132:1830–1835.
22. Walker CL, Stewart EA (2005) *Science* 308:1589–1592.
23. Fujii S, Konishi I, Horiuchi A, Orii A, Nikaido T (1999) in *Mesenchymal Cell Differentiation: Speculation About the Histogenesis of Uterine Leiomyomas* (Parthenon, New York), pp 3–15.
24. Pavlovich CP, Schmidt LS (2004) *Nat Rev Cancer* 4:381–393.
25. Fukuhara K, Kariya M, Kita M, Shime H, Kanamori T, Kosaka C, Orii A, Fujita J, Fujii S (2002) *J Clin Endocrinol Metab* 87:1729–1736.
26. Wang X, Kumar D, Seidman JD (2006) *Int J Gynecol Pathol* 25:239–242.
27. Bhattacharya N, Banerjee AK, Sengupta J (1998) *J Indian Med Assoc* 96:99.
28. Arango NA, Szotek PP, Manganaro TF, Oliva E, Donahoe PK, Teixeira J (2005) *Dev Biol* 288:276–283.
29. Szotek PP, Chang HL, Zhang L, Preffer F, Dombkowski D, Donahoe PK, Teixeira J (2007) *Stem Cells* 25:1317–1325.
30. Gargett CE (2007) *Hum Reprod Update* 13:87–101.
31. Konishi I, Fujii S, Okamura H, Mori T (1984) *J Anat* 139 (Pt 2):239–252.
32. He Q, Wan C, Li G (2007) *Stem Cells* 25:69–77.
33. Deans RJ, Moseley AB (2000) *Exp Hematol* 28:875–884.
34. Chan RW, Gargett CE (2006) *Stem Cells* 24:1529–1538.
35. Gimpl G, Fahrenholz F (2001) *Physiol Rev* 81:629–683.

The FASEB Journal • Research Communication

Human cord blood CD34 cells develop into hepatocytes in the livers of NOD/SCID/γ_c^{null} mice through cell fusion

Hisanori Fujino, Hidefumi Hiramatsu, Atsunori Tsuchiya, Akira Niwa, Haruyoshi Noma, Mitsutaka Shiota, Katsutsugu Umeda, Momoko Yoshimoto, Mamoru Ito, Toshio Heike, and Tatsutoshi Nakahata[1]

Department of Pediatrics, Graduate School of Medicine, Kyoto University, Kyoto, Japan; and the Central Institute for Experimental Animals, Kawasaki, Japan

ABSTRACT **Several studies have shown that hepatocytes can be generated from hematopoietic stem cells, but this event is believed to be rare and to require hepatic damage. To investigate this phenomenon in human cells, we used a NOD/SCID/ $_c^{null}$ (NOG) mouse model that can achieve a tremendously high level of chimerism when transplanted with human hematopoietic cells. Even without hepatotoxic treatment other than irradiation, human albumin and -1-antitrypsin-positive cells were invariably detected in the livers of NOG mice after i.v. transplantation of human cord blood CD34 cells. Human albumin was detected in the murine sera, indicating functional maturation of the human hepatocytes. Flow cytometric analysis of recipient liver cells in single-cell suspension demonstrated that human albumin-positive cells were also positive for both murine and human MHC and were negative for human CD45. PCR analysis of recipient livers revealed the expression of a wide variety of human hepatocyte- or cholangiocyte-specific mRNAs. These results show that human CD34 cells fuse with hepatocytes of NOG mice without liver injury, lose their hematopoietic phenotype, and begin hepatocyte-specific gene transcription. These phenomena were not observed when CD34 cells were transplanted. Thus, our model revealed a previously unidentified pathway of human hematopoietic stem/progenitor cell differentiation.—Fujino, H., Hiramatsu, H., Tsuchiya, A., Niwa, A., Noma, H., Shiota, M., Umeda, K., Yoshimoto, M., Ito, M., Heike, T., Nakahata, T. Human cord blood CD34 cells develop into hepatocytes in the livers of NOD/SCID/ $_c^{null}$ mice through cell fusion. *FASEB J.* 21, 3499–3510 (2007)**

Key Words: liver regeneration hematopoietic stem/progenitor cell mature hepatocyte bone marrow-derived cell

THE LIVER IS AN ORGAN WITH A NATURALLY HIGH regeneration potential. A number of hepatic cell types have been found to have regeneration potential, including liver intrinsic stem/progenitor cells, oval cells, and mature hepatocytes (1). As a general rule, the replication of existing hepatocytes is the quickest and most efficient way to generate hepatocytes for liver regeneration. In contrast, liver regeneration by oval cells takes place only when the replication of mature hepatocytes is delayed or entirely blocked, such as when acute and severe hepatocellular damage has occurred (1).

Recent studies of mice have revealed a new liver-regenerating cell type, namely, bone marrow cells. In 2000, Lagasse *et al.* (2) first showed that i.v. injection of purified bone marrow hematopoietic stem cells (c-kit^{high}Thy^{low}Lin Sca-1 cells) into mice with a lethal fumarylacetoacetate hydrolase (FAH) deficiency rescued the recipients by restoring the biochemical function of their livers; on the basis of this, they proposed the notion of "transdifferentiation," or the differentiation of hematopoietic stem cells into nonhematopoietic cells. However, in 2002 this concept of plasticity was challenged by Terada *et al.* (3) and Ying *et al.* (4), when they found that adult stem cells spontaneously fused with embryonic stem cells and took on their characteristics; these authors concluded that "cell fusion" was the mechanism of nonhematopoietic cell generation from hematopoietic cells. Studies in 2003 by Wang *et al.* (5), Vassilopoulos *et al.* (6), and Alvarez-Dolado *et al.* (7) supported the cell fusion hypothesis. However, Jang *et al.* (8) and Harris *et al.* (9) reported in 2004 that hepatocytes that differentiate from bone marrow-derived cells are not the result of cell fusion. In the same year, Willenbring *et al.* (10) and Camargo *et al.* (11) showed that hematopoietic myelomonocytic-committed cells such as macrophages are the major source of hepatocyte fusion partners. Thus, it remains unclear whether transdifferentiation or cell fusion is the main mechanism that generates hepatocytes from hematopoietic cells.

[1] Correspondence: Department of Pediatrics, Graduate School of Medicine, Kyoto University, 54 Kawahara-cho, Shogoin, Sakyo-ku, Kyoto 606-8507, Japan. E-mail: tnakaha @kuhp.kyoto-u.ac.jp

doi: 10.1096/fj.06-6109com

0892-6638/07/0021-3499 © FASEB

In humans, Alison *et al.* (12) and Theise *et al.* (13) showed that the adult human hematopoietic stem cell population can yield hepatocytes upon instruction by the appropriate environment. Korbling *et al.* (14) showed that hepatocytes are generated from the bone marrow of recipients of sex-mismatched bone marrow transplants at a high frequency that ranges from 4% to 7%. Moreover, Ng *et al.* (15) found that in human liver allografts, although most of the recipient-derived cells showed macrophage/Kupffer cell differentiation, recipient-derived hepatocytes were also present and constituted 0.62% of all the hepatocytes in the recipient.

To examine the mechanisms by which human hematopoietic cells contribute to liver regeneration, the human-to-mouse xenogeneic transplantation model was used. Several reports have shown that when human cord blood (CB) cells (all cells, CD34 cells, or CD45 cells) are injected into mice through either the portal vein or the systemic circulation, they can form human hepatocyte-like cells in the murine liver environment (16–23). However, even when there is massive liver damage, the frequency with which this hepatocytic differentiation occurs is low compared to that reported in human-to-human transplantation studies. This low level of efficiency makes it hard to clarify whether transdifferentiation or cell fusion is the primary mechanism that generates hepatocytes from human hematopoietic cells. Many attempts have been made to establish more suitable models but have met with limited success.

We postulated that the failure to achieve substantial hepatic chimerism in standard mouse models is due to *1)* the low frequency of human hematopoietic cells combined with *2)* the intrinsic immune barrier of the murine liver, which will mask the true regenerating potential of human hematopoietic cells. We previously reported that the NOD/SCID/ $_c^{null}$ mouse model provided far better human hematopoietic stem cell engraftment than did NOD/SCID and NOD/SCID/ $2m^{null}$ mice (24–26). NOD/SCID/ $_c^{null}$ mice completely lack natural killer (NK) cell activity and have dendritic cell dysfunction (24). Notably, functional human T, NK, and mast cells have been generated and matured from human hematopoietic stem cells in NOD/SCID/ $_c^{null}$ mice (25, 26).

Here we have used the NOD/SCID/ $_c^{null}$ mouse model to address questions about the regeneration of the liver from transplanted human hematopoietic stem cells. First, we asked whether human CB CD34 cells could develop into functional hepatic and cholangitic cells in the murine liver environment. Second, we asked whether the generation of hepatocytes is due to transdifferentiation or cell fusion. Third, we examined the status of human liver-specific gene transcription in the murine liver. Finally, we investigated whether CD34 cells also have the ability to produce hepatocytes. Our model proved suitable for answering these questions and revealed a previously unidentified pathway of human CD34 cell differentiation under steady-state conditions.

MATERIALS AND METHODS

Mice

NOD/SCID/ $_c^{null}$ mice were generated at the Central Institute for Experimental Animals (Kawasaki, Japan), shipped to the animal facility of Kyoto University (Kyoto, Japan), and handled with humane care under pathogen-free conditions. All experiments in this study were performed in accordance with the Animal Protection Guidelines of Kyoto University.

Cell preparation and transplantation protocol

Human CB CD34 cells were purified using a described method (25). Briefly, after we obtained informed consent from the donors parents, we collected mononuclear cells from human CB by Ficoll-Hypaque (Pharmacia, Uppsala, Sweden) density gradient centrifugation. The CD34 fraction was then isolated by using auto-MACS (Miltenyi Biotec GmbH, Bergisch Gladbach, Germany) with the "posseld2" program according to the manufacturer's recommendations. The "depl 05" and "possel" programs were added to get the CD34 fraction and the CD34 CD14 / fraction, respectively; this yielded highly pure populations. Eight- to 12-wk-old NOD/SCID/ $_c^{null}$ mice were irradiated with 240cGy, and human CB CD34 cells ($2 \ 10^4$ or $1 \ 10^5$) or CD34 CD14 / cells ($1 \ 10^7$) were injected through the tail vein. Neomycin sulfate (Invitrogen, Carlsbad, CA, USA) in acidic water was supplied to irradiated recipient mice after transplantation.

Flow cytometric analysis of peripheral blood from mice transplanted with human cells

The peripheral blood of mice was collected and transferred to ethylenediaminetetraacetic acid (EDTA) -2Na-containing CAPIJECT (Terumo Medical, Somerset, NJ, USA). The cells were then analyzed by flow cytometry (FACS caliber; BD PharMingen, San Diego, CA, USA) to measure the frequencies of various human hematopoietic cell types using the following antibodies (all purchased from BD PharMingen): fluorescein isothiocyanate- (FITC) and phycoerythrin- (PE) conjugated mouse anti-human CD3, CD4, CD8, CD14, CD19, CD33, CD45, and CD56, and allophycocyanin (APC)-conjugated rat anti-mouse CD45.

Detection of human CB-derived cells in the murine liver by immunohistochemical analysis

Mice were anesthetized, killed by cervical dislocation, and their livers were collected, fixed in 10% formalin, and embedded in paraffin blocks. Four-micrometer sections were cut and placed on silane-coated slides. After removing the paraffin with xylene, the tissue sections were rehydrated with graded alcohol, washed with water, and incubated with primary antibodies diluted with phosphate-buffered saline (PBS) or PBS containing 1% bovine serum albumin. The antibodies (and dilutions) used were rabbit anti-human albumin (1:100) (DAKO Carpinteria, CA, USA), mouse anti-human-specific hepatocyte antigen (HepPar1) (1:100) (DAKO), rabbit anti-human -1-antitrypsin (1:100) (Neomarkers, Fremont, CA, USA), mouse anti-human CD45 (1:100) (DAKO), mouse

anti-human CD68 (1:100) (DAKO), mouse anti-human mitochondria (1:100) (Chemicon International, Inc., Temecula, CA, USA), and rabbit anti-human c-met (1:100) (Santa Cruz Biotechnology, Inc., Santa Cruz, CA, USA). All antibodies except for rabbit anti-human c-met were confirmed to be specific for the relevant human antigen by immunohistochemical assays using mouse control specimens (including those from irradiated mice). Three hours incubation at room temperature or an overnight incubation at 4°C was followed by incubation with the 1:100-diluted secondary antibodies: Cy3-conjugated donkey anti-mouse IgG, FITC-conjugated donkey anti-rabbit IgG, peroxidase-conjugated donkey anti-mouse, and peroxidase-conjugated donkey anti-rabbit IgG (all purchased from Jackson ImmunoResearch Laboratories, West Grove, PA, USA). Hoechst 33324 (Molecular Probes, Eugene, OR, USA) was used for nuclear staining. Endogenous peroxidase activity was blocked by application of 3% hydrogen peroxide for 5 min at room temperature and a DAB Substrate Kit (Vector Laboratories, Burlingame, CA, USA) was used for visualization. Antigen retrieval was performed by heating the sections in 10 mM citrate or 10 mM citrate/2 mM EDTA buffer in an autoclave oven for 5 min. These prepared samples were then examined under a light or fluorescent microscope (Olympus, Tokyo, Japan).

Serum human albumin enzyme-linked immunosorbent assay (ELISA)

Peripheral blood was collected into serum separator tubes (BD PharMingen) at various points after transplantation for the human serum albumin assays, and ELISA was performed according to the manufacturer's instructions (Cygnus Technologies, Plainville, MA, USA).

Flow cytometric analysis of single liver cells obtained by collagenase perfusion

Mice were anesthetized, their abdomens were opened, and their inferior vena cava was cannulated. The hepatic vein and whole liver were then retrogradely perfused gently at 37°C with Hanks' buffered salt solution (HBSS; Gibco BRL, Grand Island, NY, USA) containing 2-[4-(2-hydroxyethyl)-1-piperazinyl]ethanesulfonic acid (HEPES) at a final concentration of 10 mM (Nakalai Tesque, Inc., Kyoto, Japan) and ethyleneglycoltetraacetic acid at a final concentration of 0.5 mmol/l. This was followed by perfusion with HBSS containing HEPES (final concentration of 10 mM) and collagenase D (final concentration of 200 g/ml) (Roche Diagnostics GmbH, Mannheim, Germany). After perfusion, a homogeneous liver cell suspension that contained hepatocytes, blood cells, and nonparenchymal cells was obtained by gentle mechanical dispersion and filtering through a 70 m nylon mesh cell strainer. After centrifugation and resuspension in PBS with 2% fetal calf serum, this preparation was characterized by flow cytometric analysis using a Cytofix/CytoPerm kit (BD PharMingen). Briefly, the cells were stained with one of the following primary antibodies: APC-conjugated mouse anti-human CD45 (BD PharMingen); FITC-, PE-, or APC-conjugated mouse anti-human HLA-ABC (BD PharMingen); or PE-conjugated rat anti-mouse H-2K^{d} (BD PharMingen). The cells were then washed, fixed, and permeabilized with Cytofix/Cytoperm solution for 20 min. After washing with Perm/Wash buffer twice, cells were incubated with isotype IgG or rabbit anti-human albumin for 30 min at 4°C, followed by incubation with FITC-conjugated donkey anti-rabbit IgG for 30 min at 4°C. After washing with Perm/Wash, the cells were analyzed by flow cytometry.

Fluorescence *in situ* hybridization (FISH)

Cy3-dUTP-labeled human genome DNA probe and Cy5-dUTP-labeled mouse genome DNA probe were used simultaneously. Slides were heated to 45°C for 30 min, then deparaffinized and dried. Slides were then denatured for 5 min in 2 saline sodium citrate (SSC) buffer, microwaved for 10 min, digested with 0.1% pepsin/0.1M HCl for 5 min, and washed with PBS. After dehydration, probes were applied and sections were incubated at 90°C for 13 min for denaturation. After overnight incubation at 37°C, the sections were stringently washed in 2 and 1 SSC containing 50% formamide. The nuclei were counterstained with 4 ,6-diamino-2-phenylindole and multicolored immunofluorescent staining was analyzed by a fluorescence microscope (Leica, Wetzlar, Germany).

Reverse transcription-polymerase chain reaction (RT-PCR)

Mice were anesthetized, then killed by cervical dislocation. Total RNA was extracted from chimeric liver, nontransplanted liver, irradiated liver, human liver, and human CB CD34 cells using Trizol reagent (Invitrogen Corp., San Diego, CA, USA) according to the manufacturer's instructions. Equal amounts of RNA from all samples were subjected to first-strand cDNA synthesis with an oligo dT primer and Superscript II RT (Invitrogen Corp.) The cDNAs were then amplified using an AmpliTaqGold Kit (Applied Biosystems, Foster City, CA, USA) and human-specific primers. Amplification was performed at 95°C for 5–10 min, followed by 30–40 cycles of 94–95°C for 30 s, 56–60°C for 30–60 s, and 72°C for 60 s, with a final extension at 72°C for 7 min. The primers and PCR reaction conditions used are detailed in **Table 1**. The PCR products were separated by electrophoresis in 1% agarose gels, stained with ethidium bromide, and photographed.

Real-time quantitative RT-PCR analysis

Forward and reverse primers as well as fluorogenic probes were designed according to Perkin-Elmer guidelines (Primer Express Software). Human glyceraldehyde 3-phosphate dehydrogenase (GAPDH) primers and probes were purchased from Applied Biosystems. Quantitative assessment of mRNA expression was performed using a human GAPDH internal standard. The expression of each mRNA was compared with each human liver mRNA expression. The primers and probes are detailed in **Table 2**.

Statistical analysis

Statistical significance was determined by using the Pearson's correlation coefficient test.

RESULTS

Large numbers of human liver parenchymal and nonparenchymal cells are present in the murine liver after human CB CD34 cell transplantation

We transplanted liver-intact NOD/SCID/ $_{c}^{null}$ mice with purified human CB CD34 cells and subjected the livers to immunohistochemical analysis at various time points to determine whether the murine livers contain hepatic cells derived from human CB CD34 cells.

TABLE 1. *The primers and PCR reaction conditions*

Genes	Primers		Annealing (°C)	Cycles
	Sense (5' to 3')	Antisense (5' to 3')		
Albumin #1	gaacttcgggatgaagggaa	gcaagtcagcaggcatctca	59	40
Albumin #2	aacgccaagtaagtgacaga	gaaaagaaaaacagatgaa	56	40
Alpha1AT	ctttgaagtcaaggacaccg	gctgaagaccttagtgatgc	56	35
Transferrin	cctgatccatgggctaagaa	ctacggaaagtgcaggcttc	58	35
RBP4	gcctctttctgcaggacaac	cgggaaaacacgaaggagta	60	40
Prealbumin	cagaaaggctgctgatgaca	caggtccactggaggagaag	59	40
CPSI	gttgtctgaaccaagcagca	cgcagtgtgcggatactaga	60	40
CYP3A4	tgtgaggaggtagatttggctc	tcaggaggagttaatggtgctaa	59	40
TAT	cgcagattactcccttgctc	gtgtccccaacttctttcca	58	40
TO	tgcagcagttttccattctg	tcagccacctgttcctcttt	56	40
FVIII	tgccacaactcagactttcg	gtcgcaagagcatcaacaaa	56	40
CK7	caggaactcatgagcgtgaa	gggtgggaatcttcttgtga	58	40
CK19	aggtggattccgctccgggca	atcttcctgtccctcgagca	58	40
eNOS	tgctggcatacaggactcag	taggtcttggggttgtcagg	59	40
Human HPRT	aattatggacaggactgaacgtc	cgtggggtccttttcaccagcaag	60	35
Mouse HPRT	gctggtgaaaaggacctct	cacaggactagaacacctgc	59	30

TABLE 2. *Primers and probes for real-time quantitative RT-PCR*

Genes	Primers		Probes
	Sense (5' to 3')	Antisense (5' to 3')	
Albumin	ttaccaaagtccacacggaatg	caaggtccgccctgtcat	tgccatggagatctgcttgaatgtgct
CK7	gcgtgagtaccaggaactcatg	gcttgcggtaggtggcg	tgaagctggccctggacatcgaga
CPSI	ggcaatgctttccacagga	ttggccggaatgattgct	agataccccagaaaggcatcctgataggcat
TAT	gactcgggcaaatataatggct	gcaatctcctcccgactgg	tgccccatccatcggcttcc

TABLE 3. *Correlation between frequency of human albumin-positive cells by immunohistochemistry and the levels of human albumin in the blood of recipient mice*

Mouse	Time after transplantation	Frequency of human albumin-positive cells by immunohistochemistry (%)	Serum human albumin (g/ml)
#1	3 months	1.67(17/1019)	0.8
#2	3 months	2.15(22/1023)	0.6
#3	5 months	2.56(28/1094)	1.4
#4	5 months	2.61(33/1263)	2.3
#5	6 months	3.43(32/933)	3.7

Human albumin-expressing cells were invariably found in the livers of all the recipient mice. Some formed large clusters around the portal veins (**Fig. 1A**) whereas others were scattered throughout the liver lobule and showed a punctuate distribution away from the portal veins (Fig. 1*B*). Double staining for human albumin and human-specific hepatocyte antigen (HepPar1) revealed that the human albumin-positive cells were also HepPar1-positive (Fig. 1*C, D*).

Because the liver contains a large amount of peripheral blood, we checked the distribution of human peripheral blood cells. Double staining of the liver sections for human CD45 and human albumin revealed small, round, human CD45-positive peripheral blood cells beneath the basal membrane of the portal veins and in the sinusoidal area of the livers (Fig. 1*E, F*); an anti-human albumin antibody stained a different population of cells in the same section. We also detected human -1-antitrypsin-positive cells in the liver (Fig. 1*H*), which indicates the functional maturation of human CB-derived hepatocytes; these cells were also present in a section of human liver used as a positive control (Fig. 1*G*). These hepatocytes were first detected 1 month after transplantation and tended to increase in number with time (data not shown).

Kupffer cells are spindle-shaped; they are located between hepatocytes and retain macrophage markers such as CD68 (27) (**Fig. 2A**). Mature human Kupffer cells were present in the murine liver environment of the recipient mice (Fig. 2*B*). Murine Kupffer cells were not stained by anti-human CD68 antibody (Fig. 2*C*).

We assessed the ability of human CB CD34 cells to

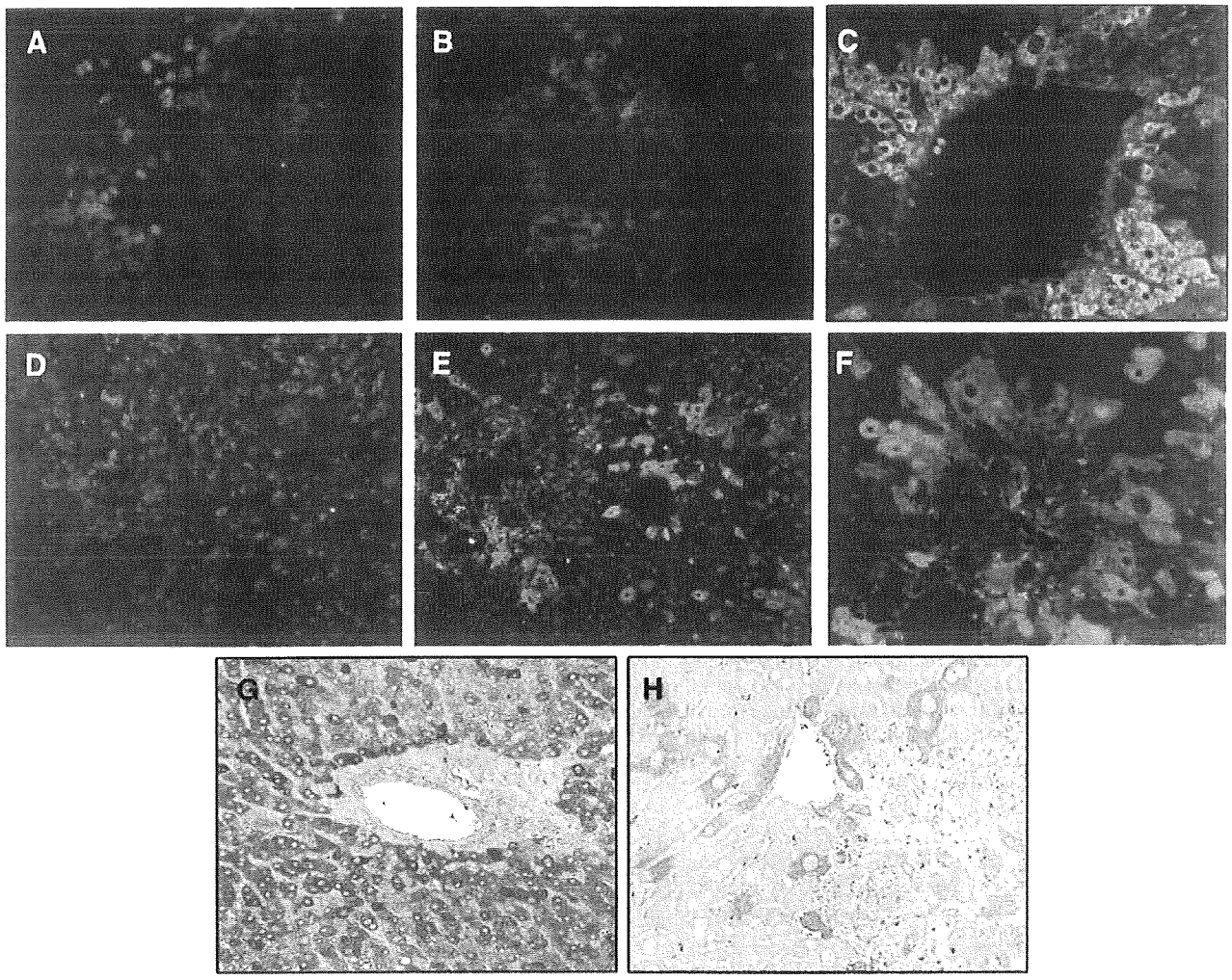

Figure 1. Large numbers of human CB CD34 cell-derived liver parenchymal cells are found in the livers of recipient mice. *A, B)* Human albumin-expressing cells in murine liver sections were identified using an FITC-labeled anti-human albumin antibody. *C, D)* Triple staining of murine liver sections for human albumin (green), human HepParl (red) and nuclei (blue). *E, F)* Triple staining of murine liver sections for human albumin (green), human CD45 (red), and nuclei (blue). *G)* Immunohistochemical analysis of a human liver section as a positive control for human -1-antitrypsin staining. *H)* Identification of human -1-antitrypsin-expressing cells in transplanted murine liver sections.

produce cholangiocytes by immunohistochemistry with antibodies for human mitochondria and c-met. The antibody for c-met is reported to recognize both hepatocytes and cholangiocytes, particularly when they are proliferating (28, 29). Cube-shaped cholangiocytic cells in the recipient livers were positive for human mitochondria and c-met, which suggests that these cells are of human origin (Fig. 2*D–F*). Indeed, we identified 250 portal areas from 10 independent mice and found three ducts containing human marker (human mitochondria).

To exclude the possibility that 240cGy radiation might induce liver injury, we evaluated the liver after radiation. Histology showed no liver damages such as inflammation, lobar necrosis, or fibrosis. We could not detect TUNEL (TdT-mediated dUTP-biotin nick end labeling)-positive cells. Furthermore, serum AST/ALT levels did not increase (data not shown).

These results indicate that human CD34 cells can produce human hepatocytes, Kupffer cells, and cholangiocytes in the murine liver environment; these cells develop even in the absence of massive hepatotoxic damage.

Human albumin is present in the peripheral blood of recipient mice and increases with time after transplantation

To check whether the human albumin-positive cells in the livers of recipient mice have the ability to secrete albumin into the murine bloodstream, we measured levels of human albumin in the blood of recipient mice by ELISA at various points after the transplantation. We could not detect human albumin at all in the peripheral blood of either untransplanted mice (n 5) or mice within 2 months after transplantation (n 5) (**Fig. 3*A***

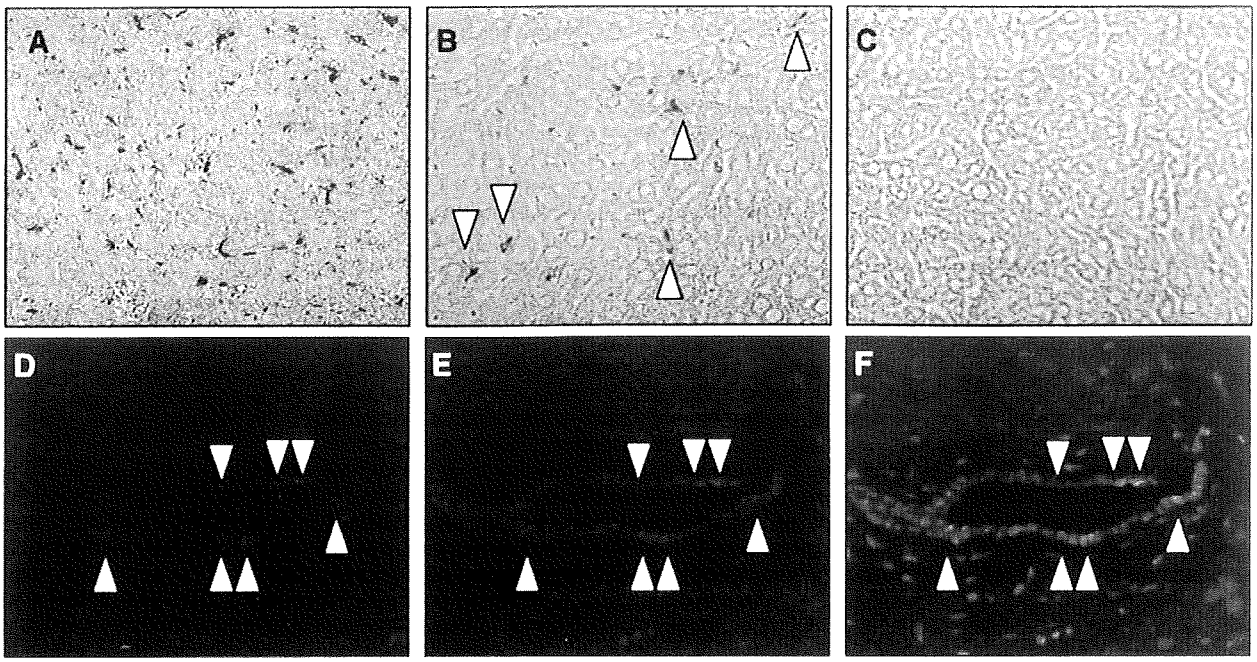

Figure 2. Kupffer cells and cholangiocytes derived from human CB CD34 cells are present in the transplanted murine liver. *A)* Immunohistochemical analysis of a human liver section as a positive control for human CD68 staining. *B)* Liver sections of a recipient mouse. Human CD68-expressing cells were identified by staining with an HRP-labeled anti-human CD68 antibody. *C)* Murine Kupffer cells were not stained by anti-human CD68 antibody. *D, F)* Liver sections from recipient mice were analyzed for the presence of human mitochondria-positive cells (stained red, *D)* and human or mouse c-met-positive cells (green, *E*). The two images in panels *D, E* are merged in panel *F*. Arrowheads indicate the human mitochondria-positive cells. Nuclei are stained blue.

and data not shown). Serum human albumin was first detected 3 months after transplantation, and the levels increased gradually with time after transplantation. In addition, the human albumin levels increased in all four mice whose levels we measured serially (Fig. 3*A*). These results indicate that human CB CD34 cells can generate human albumin-positive cells continuously in the murine liver and that these cells become mature enough to secrete albumin from their cytoplasm into the bloodstream. Indeed, we found a positive correlation between the frequency of human albumin-positive cells determined by immunohistochemistry and levels of human albumin in the blood of recipient mice (Table 3).

Human albumin levels in the peripheral blood of recipient mice correlate with the degree of peripheral blood chimerism and human T cell frequencies

Using flow cytometry, we detected various types of human hematopoietic cells in the peripheral blood of the recipient mice, including T cells (CD3 , CD4 , CD8), B cells (CD19), myelomonocytic cells (CD14 , CD33), and NK cells (CD56) (Fig. 3*B* and data not shown). This is consistent with previously reports (24, 25). We examined whether the human CB CD34 cells first give rise to a particular hematopoietic cell population in the peripheral blood and then participate in producing the human cell-derived hepatocytes in the recipient mice. To address this question, we first asked whether the chimerism of the liver in the recipient mice (defined as the levels of human albumin in the serum) correlated with the chimerism of the whole peripheral blood cell population (defined as the percentage of human CD45 cells relative to all mouse and human CD45 cells). We found a strong positive correlation between the chimerism of the liver and the whole peripheral blood cell population (Fig. 3*C*). We then examined whether the liver chimerism correlated with the percentages of particular types of human leukocytes in the peripheral blood. We found that the percentage of human T cells (human CD3 cells) most strongly correlated with the levels of human albumin in the serum (Fig. 3*D*). The percentage of human myelomonocytic cells [defined as either human CD45 minus (CD3 plus CD19) or human CD14] correlated weakly with the human albumin levels (Fig. 3*D* and data not shown). In contrast, the human albumin levels did not correlate with human B cell (human CD19) frequency (Fig. 3*D*).

Human albumin-positive cells in the livers of recipient mice express both human and mouse markers, suggesting that cell fusion occurs

We next characterized the human hepatocytes and blood cells in the recipient mice by assessing their expression of various surface markers and intracellular

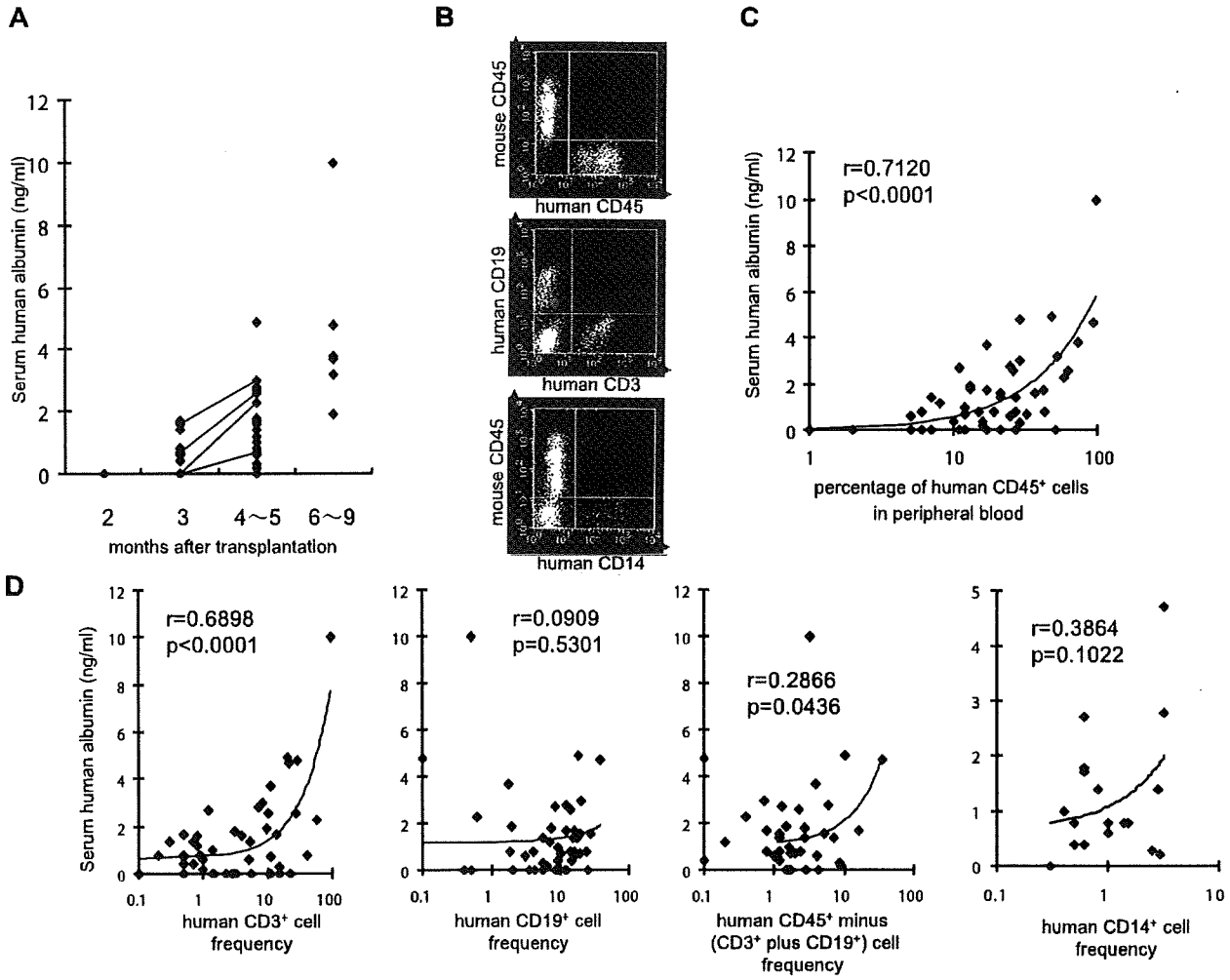

Figure 3. Levels of human albumin in the blood of recipient mice correlate with time after transplantation, the degree of overall peripheral blood chimerism, and human CD3 T cell frequencies. *A)* Serum human albumin was detected by ELISA for the first time 3 months after transplantation. Human albumin levels in the peripheral blood of recipient mice increased gradually with time after transplantation. The bars connecting the symbols indicate serial measurements in the same mice. *B)* The peripheral blood of the recipient mice contained a variety of human cells. *C)* Relationship between the human albumin levels in the peripheral blood and the chimerism of the peripheral blood. The regression line is indicated. *D)* The relationship between the human albumin levels in the peripheral blood and the percentage of human CD3 T cells, human CD19 B cells, and myelomonocytic cells (human CD45 minus [CD3 plus CD19] cells or CD14 cells).

proteins by flow cytometry. We first obtained cells from the liver by two-step collagenase perfusion at least 3 months after the transplantation (**Fig. 4***A*). When the dissociated cells from untransplanted control mice were plotted on the basis of their forward scatter and side scatter, we identified two regions: R1 and R2 (Fig. 4*B*). R1 contained mature hepatocytes whereas R2 contained CD45 hematopoietic cells (data not shown). For the recipient mice, 0.88% to 4.73% of the cells in R1 (mean 2.73%) were positive for human albumin (see R4 in Fig. 4*C, D*). These human albumin-positive cells were distinguishable from the human CD45 hematopoietic cells (see R5 in Fig. 4*C*). We confirmed that the human albumin-positive cells and human CD45 cells expressed human HLA-ABC (Fig. 4*E*). Staining with an anti-mouse H-2K^d antibody revealed that the human albumin-positive cells also expressed the murine MHC class I molecule (Fig. 4*F*). In contrast, human CD45 cells in the liver were negative for mouse H-2K^d (Fig. 4*G*). These data suggest that the human albumin-positive hepatocytes in this model were produced by cell fusion.

The livers of recipient mice contain nucleus positive for both human and mouse genomic DNAs

To clarify the genetic content of the human albumin-positive hepatocytes, we performed FISH for human

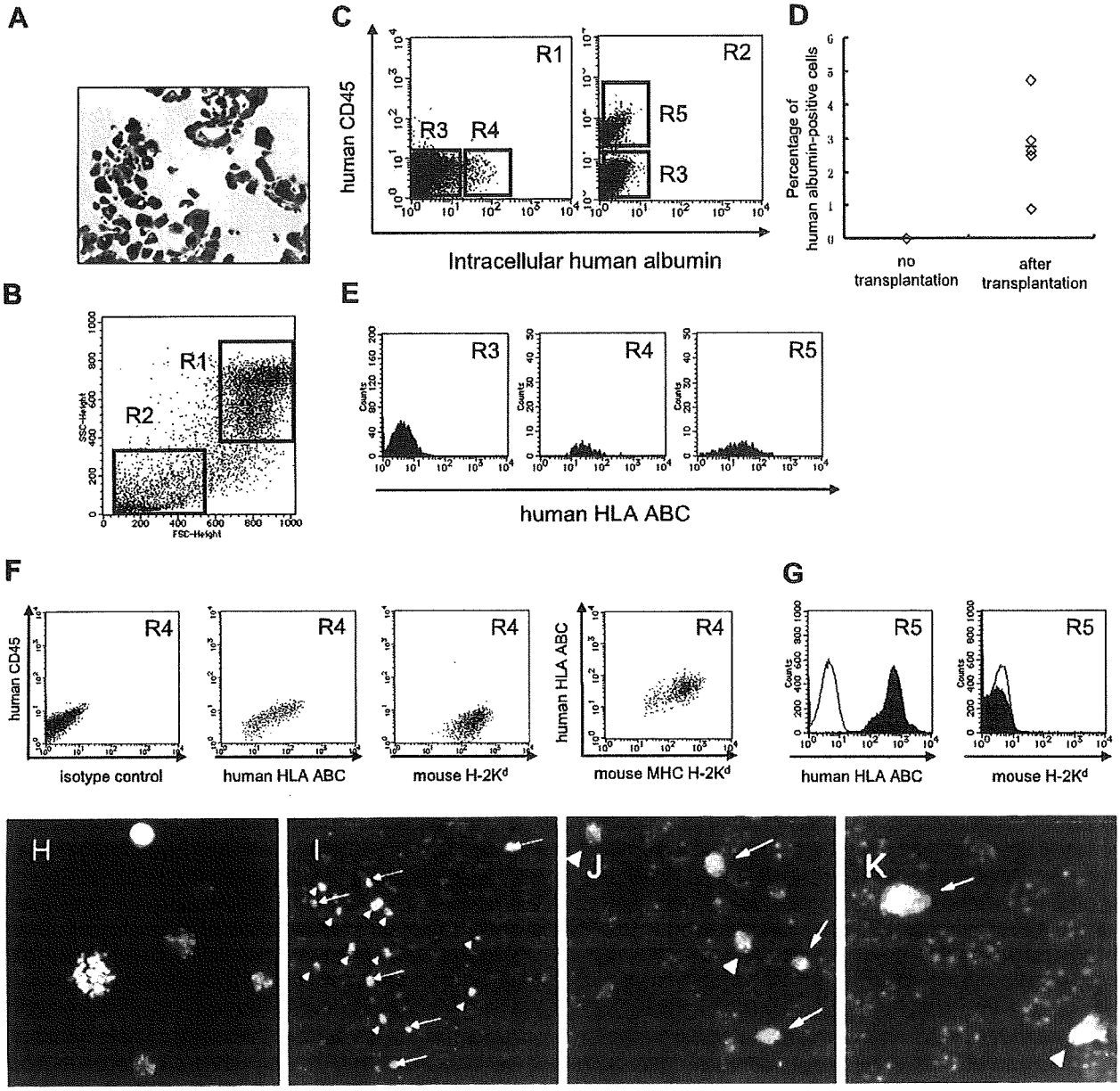

Figure 4. Human CB-derived albumin-positive hepatocytes possess both human and mouse markers, suggesting that cell fusion occurs. *A)* The murine liver after collagenase perfusion. Single cells of various sizes and shapes were acquired. *B)* Flow cytometric analysis of the dissociated liver cells. These cells were divided into two types on the basis of their size and granularity, as shown by regions R1 and R2. *C)* Staining of the dissociated liver cells from recipient mice with anti-human CD45 and anti-human albumin antibodies resulted in three regions: double-negative cells (R3), human albumin-positive cells (R4), and human CD45 cells (R5). Note that the human albumin-positive cells belong to R1 whereas the human CD45 cells belong to R2. *D)* The percentage of liver cells from recipient mice that were human albumin-positive in R1 ranged from 0.88% to 4.73%. *E)* Analysis of human HLA-ABC expression by the cells in R3, R4, and R5. The cells in both R4 and R5 express human HLA-ABC whereas the cells in R3 do not. *F)* Analysis of human HLA-ABC and mouse H-2K^d expression by human albumin-positive cells. Note that these cells expressed both human and murine MHC class I molecules. *G)* Analysis of human HLA-ABC and mouse H-2K^d expression by human CD45-positive cells. These cells expressed the human MHC class I molecule but not the murine MHC class I molecule. *H)* Verification of human (yellow) and mouse (red)-specific genomic DNA probe. *I–K)* Triple staining of murine liver sections for human DNA (yellow), mouse DNA (red), and nuclei (blue). Arrows indicate the presence of fusion-derived nuclei. The nuclei of human peripheral blood cells were also identified (arrowheads).

and mouse genomic DNA. Figure 4*H* illustrates the verification of probes on a test specimen. Figure 4*I–K* demonstrates detection of human and mouse genomic DNA on the livers of recipient mice, revealing the presence of a single nucleus positive for both human and mouse genome. The percentage of these nuclei ranged from 2 to 5%, similar to the frequency of human albumin-positive cells determined by immuno-

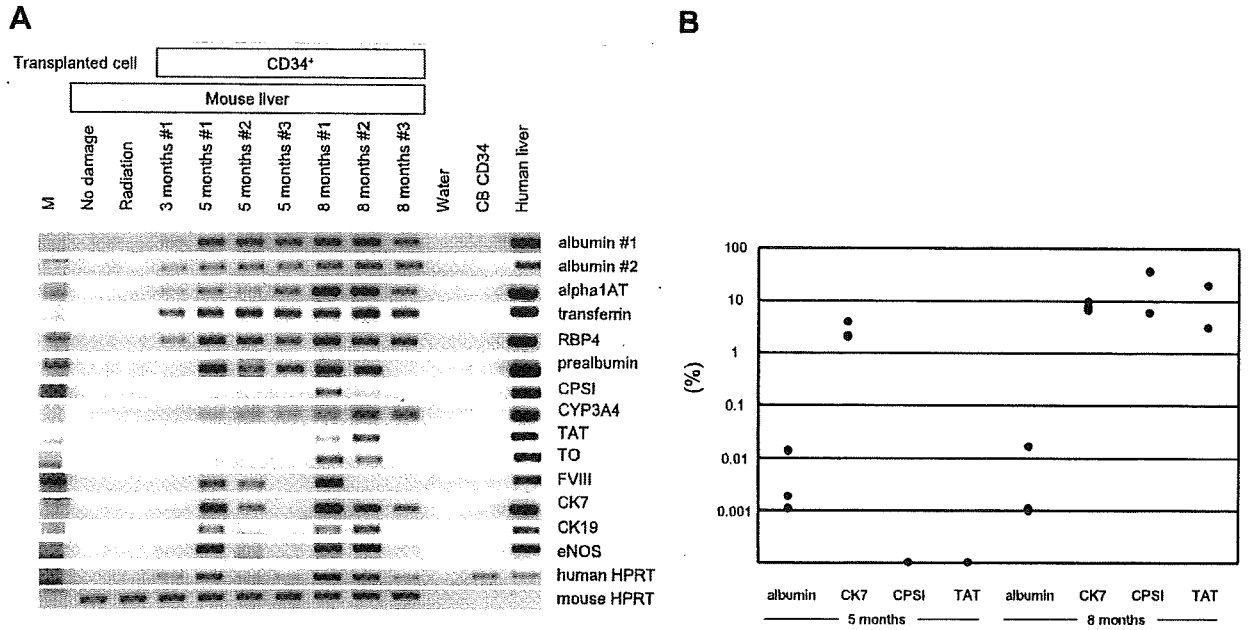

Figure 5. Up-regulation of a wide variety of human liver-specific mRNAs in the livers of human CB CD34 -recipient mice. *A)* M, size marker; radiation, 240cGy radiation; 1 AT, -1-antitrypsin; RBP4, retinol binding protein 4; CPSI, carbamoyl phosphate synthetase I; TAT, tyrosine aminotransferase; TO, tryptophan-2,3-dioxygenase; FVIII, coagulation factor VIII; CK7, cytokeratin 7; CK19, cytokeratin 19; eNOS, endothelial nitric oxide synthase; HPRT, hypoxanthine guanine phosphoribosyl transferase. Chimeric samples were collected at the indicated time points after transplantation. *B)* Real-time quantitative RT-PCR analysis. The comparative cycle threshold (C_T) method was used to determine the relative expression levels of human albumin, CK7, CPSI, and TAT. The threshold cycles for each gene and human GAPDH were determined and the cycle number difference (C_T) was calculated for each replicate. Relative expression values were calculated using the mean of C_T from the 3 replicates and expressed as $2^{(\ CT)}$.

histochemistry. These data showed that nuclear fusion occurred in the livers of recipient mice.

A wide variety of human liver-specific mRNAs are transcribed in the CB-derived human hepatocytes in the murine liver

We next used RT-PCR to analyze the murine liver for the presence of human albumin mRNAs after human CB CD34 cell transplantation into liver-intact mice (**Fig. 5*A***). We first used two different primer pairs to assess the presence of human albumin mRNA, which we detected in the livers of all seven mice transplanted with human CB CD34 cells. We confirmed that neither the livers of untransplanted mice nor human CB CD34 cells expressed human albumin mRNA. Human albumin mRNAs were expressed just 1 month after transplantation (data not shown).

We then examined the samples for mRNA expression of other human hepatic parenchymal and nonparenchymal markers. To our surprise, we found that a wide variety of human liver-specific mRNAs were newly transcribed: human -1-antitrypsin (1AT), transferrin and retinol binding protein 4 (RBP4) and prealbumin (all of which are rapid turnover proteins), carbamoyl phosphate synthetase I (CPSI), CYP3A4, tyrosine aminotransferase (TAT) and tryptophan-2,3-dioxygenase (TO) (all of which serve as terminal hepatic differentiation markers), coagulation factor VIII (FVIII), cytokeratin 7 (CK7), cytokeratin 19 (CK19), and endothelial nitric oxide synthase (eNOS). All of these genes were expressed in the livers of the recipient mice in the absence of any liver damage. We also found that human CK18 mRNA (mature hepatocyte marker; ref. 21) was newly transcribed in the livers of all seven mice transplanted, although we found that CB CD34 cells also expressed it (data not shown). It is notable that, as with albumin, the percentage of mice with livers bearing human liver-specific mRNA tended to rise with time after transplantation. Furthermore, using real-time quantitative RT-PCR analysis, we confirmed expression levels of the human albumin, CK7, CPS1, and TAT in chimeric livers (Fig. 5*B*). The levels of these genes also tended to rise higher with time after transplantation, and some exceeded 10% compared with those of human livers. These data indicate that human CB CD34 cells, which are initially destined to become mature blood cells, begin human liver-specific gene transcription in the murine liver through cell fusion.

Human CB CD34 cells can develop into human albumin-positive hepatocytes whereas CD34 cells cannot

To test whether CD34 cells can develop into mature hepatocytes in the murine liver as CD34 cells do, we

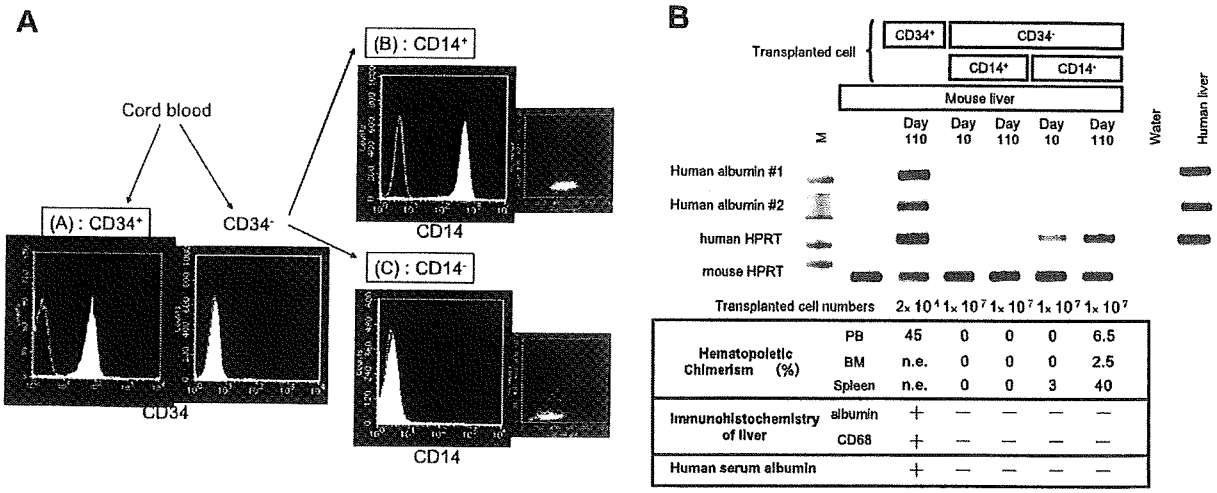

Figure 6. Comparison of the hepatocyte-producing ability of human CB CD34 and CD34 cells. *A)* Depiction of the process used to prepare the transplantable cell populations and analysis of their purity by flow cytometry. *B)* CD34 cells generated high numbers of human blood cells and human albumin-positive cells (as shown by immunohistochemistry) as well as considerable amounts of human albumin mRNA levels in the liver (as shown by RT-PCR) and human albumin protein levels in the murine bloodstream, whereas CD34 cells did not. Each column in the table refers to the lane directly above it. M, size marker; n.e., not examined.

sorted the CB from the same donor into three populations and injected each i.v. into NOD/SCID/ $_c^{null}$ mice: *1)* CD34 cells, *2)* CD34 CD14 cells (monocytes), and *3)* CD34 CD14 cells (T cells, B cells, NK cells, mesenchymal stem cells (MSCs), and others). A flow cytometric analysis showed that contamination of the CD34 groups with CD34 cells was negligible and that the CD14 and CD14 cells were efficiently separated by cell sorting (**Fig. 6A**). Although 2 10^4 CD34 cells generated large numbers of functional hematopoietic and hepatic cells that expressed human markers, no human albumin expression was detected in the liver at either day 10 or day 110 when 1 10^7 CD34 14 or CD34 14 cells were transplanted (500-fold the CD34 cell dose) (Fig. 6*B*). In the case of CD34 14 cells transplantation, significant hematopoietic chimerism came from temporarily expanding donor T cells. Indeed, all the hematopoietic cells in these mice are CD3 positive. These results clearly show that only human CB CD34 cells, and not CD34 cells, can generate human albumin-expressing cells in the livers of recipient mice in our model.

DISCUSSION

Lagasse *et al.* (2) were the first to demonstrate that purified hematopoietic stem cells can differentiate into hepatocytes *in vivo.* Subsequently, congenic mouse-to-mouse transplantation of bone marrow populations rich in hematopoietic stem cells was used to show hepatic differentiation of hematopoietic cells. However, it is controversial how hematopoietic stem cells generate hepatocytes. Many researchers have used the human-to-mouse xenogeneic transplantation model, but with extremely low efficiency (0.5%), making it difficult to analyze the mechanism by which hematopoietic stem cell transplantation induces liver regeneration. We previously demonstrated that NOD/SCID/ $_c^{null}$ mice show superior efficient human hematopoietic stem cell engraftment (24, 25). In the current study, small numbers of CD34 cells (which represent hematopoietic stem cells) were transplanted to exclude the effects of other cells types (*e.g.*, the CD34 MSCs and other unknown stem cells). We demonstrated that the livers of the recipient mice expressed human albumin, HepPar1, and -1-antitrypsin protein. In addition, we detected considerable numbers of human albumin-positive cells (an average of 2.73% of the total number of hepatocytes) by flow cytometry. These numbers are close to the numbers detected in the clinical human-to-human transplantation cases. We also detected human albumin in the murine bloodstream. Finally, we revealed that livers of the recipient mice express a variety of human liver-specific genes. These findings suggest that functional human hepatic cells develop in the liver after transplantation of human CB CD34 cells into liver-intact NOD/SCID/ $_c^{null}$ mice.

Results showing that *1)* the human albumin-positive hepatocytes expressed not only human HLA-ABC, but also mouse H-2K^d, and that *2)* the livers of recipient mice contained nucleus positive for both human and mouse genomic DNAs strongly support not transdifferentiation, but cell fusion, as the main mechanism of this phenomenon. This appears to contrast with the conclusions drawn from some other human-to-mouse models (16, 19). It is possible that, in our model, the human hematopoietic cells are abundantly supplied from bone marrow to the systemic circulation, and that

they infiltrate the liver and have more opportunity to develop into functional human hepatic cells through cell fusion due to the far better human hematopoietic stem cell engraftment.

We found that human albumin levels in the peripheral blood correlated strongly with the overall peripheral blood chimerism and the numbers of human T cells in the peripheral blood, but correlated weakly with the numbers of human myelomonocytic cells in the peripheral blood. However, our short-term and long-term observations revealed that neither CD34 CD14 cells (monocytes) nor CD34 CD14 cells (T cells, B cells, NK cells, MSCs, and others) could produce albumin-positive cells. This shows that although these terminally differentiated human cells (T cells and myelomonocytic cells) or MSCs may contribute to human liver regeneration indirectly, each alone might be insufficient to become a direct fusion partner. Previous studies have shown that myelomonocytic cells are sufficient for generating hepatocytes in mouse cells (10, 11). Selzner *et al.* (30) also proposed that Kupffer cells, which reside in the sinusoids and produce cytokines, recruit other cells or release TNF- and IL-6, which then initiate hepatocyte proliferation *in vivo*. Some of our findings support the possibility that myelomonocytic cells or Kupffer cells may to some extent drive the production of human albumin-positive hepatocytes: we detected a weak positive correlation between human myelomonocytic cells and human albumin levels, and detected human CD68 Kupffer cells in the transplanted murine livers. However, our data showed that *1)* human CB CD34 CD14 cells alone did not develop into human albumin-positive cells, and *2)* many of the human albumin-positive cells we detected by immunohistochemistry were not located adjacent to CD68 Kupffer cells (data not shown). These observations may suggest that the production of human albumin-positive cells, at least in our model, cannot be explained merely by direct cell fusion between myelomonocytic cells/Kupffer cells and hepatocytes, as has been shown in mouse-to-mouse transplantation studies (10, 11). Nevertheless, our experiment cannot exclude the possibility that differentiated progeny of human hematopoietic stem cells fuse with hepatocytes, considering the very long lag time between transplantation of CD34 cells and the increase in albumin levels. If we transplanted more cells or chose a different mode of transplantation, we could achieve a more efficient deposition of cells in the liver and could detect the fusion of infused human cells. Recently, Manz *et al.* (31) showed the prospective isolation of the human clonogenic common myeloid progenitors and their downstream progeny. The transplantation of highly purified hematopoietic intermediates helps us to better understand the ability to fuse them with hepatocytes.

A striking observation from our study is that CB CD34 cells are transcriptionally converted into liver cells after entering the liver of NOD/SCID/ $_c^{null}$ mice even in the absence of damage-associated stimuli other than a small dose of total body irradiation (with which the mice are preconditioned prior to transplantation). It is generally believed that tissue damage is indispensable for the hematopoietic-to-hepatic cell lineage transition (1) except for the FAH mouse model (32). However, we found that even without massive liver damage, human CB CD34 cells or their progeny cells could fuse with hepatocytes of NOD/SCID/ $_c^{null}$ mouse, lose their hematopoietic surface markers (CD45), and up-regulate human liver-specific gene transcription, contrary to other human-to-mouse xenogeneic transplantation models (17, 18, 20–23). There may be several reasons why a wide variety of human hepatocyte-specific genes are so efficiently transcribed and translated in our liver-intact NOD/SCID/ $_c^{null}$ mouse model. First, the NOD/SCID/ $_c^{null}$ mice may provide murine liver-specific transcription factors that promote human liver-specific gene transcription. It is possible that different strains of xenograft recipients may have different liver environments with respect to liver-specific transcription factors and that these differences influence the efficiency with which human cells with different properties are developed. Second, the observation that human albumin levels in the peripheral blood correlated strongly with human CD3 T cell levels suggests that these human T cells in murine liver may, not directly but indirectly, induce the hepatocyte development pathway *in vivo*. Further study is needed to clarify how the transcription of liver-specific genes is up-regulated in nuclei once cells are committed to a hematopoietic lineage. In our model, it took several months to up-regulate mature liver-specific genes. One explanation for the delay in hepatocyte gene activation is that in the case of donor-derived cells emerging around portal veins, cell fusion might have occurred with a progenitor cell, and thus maturation happened slowly.

We transplanted CB CD34 cells into NOD/SCID/ $_c^{null}$ mice without irradiation but could not observe either hematopoietic engraftment or human hepatocytes in the liver of recipient mice. Therefore, we could not determine the influence of radiation on the frequency of cell fusion. With regard to the human albumin level in the peripheral blood of recipient mice, levels would be expected to be in micrograms per milliliter, not only nanograms per milliliter. Human albumin mRNA levels quantitated by real-time PCR were also low. There seem to be additional factors that control production and secretion of the albumin into the bloodstream of the mice. This awaits further investigation.

Using immunohistochemistry, we also showed that some cholangiocytes express human markers (human mitochondria). Whether this hematopoietic-to-cholangiocytic transition is due to transdifferentiation or cell fusion remains to be elucidated.

In conclusion, we have established a new model of efficient hematopoietic-to-nonhematopoietic transition. This experimental model system allows the formation of relatively large numbers of human-derived hepatic cells under near-physiological conditions, a

valuable tool for investigating the development of functional human hepatic cells from hematopoietic cells. Further elucidation of the molecular mechanisms by which blood cells efficiently become liver cells will greatly promote the feasibility of using conventional hematopoietic stem cell transplantation to treat patients with liver dysfunction. FJ

REFERENCES

1. Fausto, N. (2004) Liver regeneration and repair: hepatocytes, progenitor cells, and stem cells. *Hepatology* **39,** 1477–1487
2. Lagasse, E., Connors, H., Al-Dhalimy, M., Reitsma, M., Dohse, M., Osborne, L., Wang, X., Finegold, M., Weissman, I. L., and Grompe, M. (2000) Purified hematopoietic stem cells can differentiate into hepatocytes in vivo. *Nat. Med.* **6,** 1229–1234
3. Terada, N., Hamazaki, T., Oka, M., Hoki, M., Mastalerz, D. M., Nakano, Y., Meyer, E. M., Morel, L., Petersen, B. E., and Scott, E. W. (2002) Bone marrow cells adopt the phenotype of other cells by spontaneous cell fusion. *Nature* **416,** 542–545
4. Ying, Q. L., Nichols, J., Evans, E. P., and Smith, A. G. (2002) Changing potency by spontaneous fusion. *Nature* **416,** 545–548
5. Wang, X., Willenbring, H., Akkari, Y., Torimaru, Y., Foster, M., Al-Dhalimy, M., Lagasse, E., Finegold, M., Olson, S., and Grompe, M. (2003) Cell fusion is the principal source of bone-marrow-derived hepatocytes. *Nature* **422,** 897–901
6. Vassilopoulos, G., Wang, P. R., and Russell, D. W. (2003) Transplanted bone marrow regenerates liver by cell fusion. *Nature* **422,** 901–904
7. Alvarez-Dolado, M., Pardal, R., Garcia-Verdugo, J. M., Fike, J. R., Lee, H. O., Pfeffer, K., Lois, C., Morrison, S. J., and Alvarez-Buylla, A. (2003) Fusion of bone-marrow-derived cells with Purkinje neurons, cardiomyocytes and hepatocytes. *Nature* **425,** 968–973
8. Jang, Y. Y., Collector, M. I., Baylin, S. B., Diehl, A. M., and Sharkis, S. J. (2004) Hematopoietic stem cells convert into liver cells within days without fusion. *Nat. Cell Biol.* **6,** 532–539
9. Harris, R. G., Herzog, E. L., Bruscia, E. M., Grove, J. E., Van Arnam, J. S., and Krause, D. S. (2004) Lack of a fusion requirement for development of bone marrow-derived epithelia. *Science* **305,** 90–93
10. Willenbring, H., Bailey, A. S., Foster, M., Akkari, Y., Dorrell, C., Olson, S., Finegold, M., Fleming, W. H., and Grompe, M. (2004) Myelomonocytic cells are sufficient for therapeutic cell fusion in liver. *Nat. Med.* **10,** 744–748
11. Camargo, F. D., Finegold, M., and Goodell, M. A. (2004) Hematopoietic myelomonocytic cells are the major source of hepatocyte fusion partners. *J. Clin. Invest.* **113,** 1266–1270
12. Alison, M. R., Poulsom, R., Jeffery, R., Dhillon, A. P., Quaglia, A., Jacob, J., Novelli, M., Prentice, G., Williamson, J., and Wright, N. A. (2000) Hepatocytes from non-hepatic adult stem cells. *Nature* **406,** 257
13. Theise, N. D., Nimmakayalu, M., Gardner, R., Illei, P. B., Morgan, G., Teperman, L., Henegariu, O., and Krause, D. S. (2000) Liver from bone marrow in humans. *Hepatology* **32,** 11–16
14. Korbling, M., Katz, R. L., Khanna, A., Ruifrok, A. C., Rondon, G., Albitar, M., Champlin, R. E., and Estrov, Z. (2002) Hepatocytes and epithelial cells of donor origin in recipients of peripheral-blood stem cells. *N. Engl. J. Med.* **346,** 738–746
15. Ng, I. O., Chan, K. L., Shek, W. H., Lee, J. M., Fong, D. Y., Lo, C. M., and Fan, S. T. (2003) High frequency of chimerism in transplanted livers. *Hepatology* **38,** 989–998
16. Ishikawa, F., Drake, C. J., Yang, S., Fleming, P., Minamiguchi, H., Visconti, R. P., Crosby, C. V., Argraves, W. S., Harada, M., Key, L. L., Jr., Livingston, A. G., Wingard, J. R., and Ogawa, M. (2003) Transplanted human cord blood cells give rise to hepatocytes in engrafted mice. *Ann. N. Y. Acad. Sci.* **996,** 174–185
17. Kakinuma, S., Tanaka, Y., Chinzei, R., Watanabe, M., Shimizu-Saito, K., Hara, Y., Teramoto, K., Arii, S., Sato, C., Takase, K., Yasumizu, T., and Teraoka, H. (2003) Human umbilical cord blood as a source of transplantable hepatic progenitor cells. *Stem Cells* **21,** 217–227
18. Kollet, O., Shivtiel, S., Chen, Y. Q., Suriawinata, J., Thung, S. N., Dabeva, M. D., Kahn, J., Spiegel, A., Dar, A., Samira, S., *et al.* (2003) HGF, SDF-1, and MMP-9 are involved in stress-induced human CD34 stem cell recruitment to the liver. *J. Clin. Invest.* **112,** 160–169
19. Newsome, P. N., Johannessen, I., Boyle, S., Dalakas, E., McAulay, K. A., Samuel, K., Rae, F., Forrester, L., Turner, M. L., Hayes, P. C., Harrison, D. J., Bickmore, W. A., and Plevris, J. N. (2003) Human cord blood-derived cells can differentiate into hepatocytes in the mouse liver with no evidence of cellular fusion. *Gastroenterology* **124,** 1891–1900
20. Nonome, K., Li, X. K., Takahara, T., Kitazawa, Y., Funeshima, N., Yata, Y., Xue, F., Kanayama, M., Shinno, E., Kuwae, C., Saito, S., Watanabe, A., and Sugiyama, T. (2005) Human umbilical cord blood-derived cells differentiate into hepatocyte-like cells in the Fas-mediated liver injury model. *Am. J. Physiol.* **289,** G1091–G1099
21. Sharma, A. D., Cantz, T., Richter, R., Eckert, K., Henschler, R., Wilkens, L., Jochheim-Richter, A., Arseniev, L., and Ott, M. (2005) Human cord blood stem cells generate human cytokeratin 18-negative hepatocyte-like cells in injured mouse liver. *Am. J. Pathol.* **167,** 555–564
22. Tanabe, Y., Tajima, F., Nakamura, Y., Shibasaki, E., Wakejima, M., Shimomura, T., Murai, R., Murawaki, Y., Hashiguchi, K., Kanbe, T., *et al.* (2004) Analyses to clarify rich fractions in hepatic progenitor cells from human umbilical cord blood and cell fusion. *Biochem. Biophys. Res. Commun.* **324,** 711–718
23. Wang, X., Ge, S., McNamara, G., Hao, Q. L., Crooks, G. M., and Nolta, J. A. (2003) Albumin-expressing hepatocyte-like cells develop in the livers of immune-deficient mice that received transplants of highly purified human hematopoietic stem cells. *Blood* **101,** 4201–4208
24. Ito, M., Hiramatsu, H., Kobayashi, K., Suzue, K., Kawahata, M., Hioki, K., Ueyama, Y., Koyanagi, Y., Sugamura, K., Tsuji, K., Heike, T., and Nakahata, T. (2002) NOD/SCID/gamma(c)(null) mouse: an excellent recipient mouse model for engraftment of human cells. *Blood* **100,** 3175–3182
25. Hiramatsu, H., Nishikomori, R., Heike, T., Ito, M., Kobayashi, K., Katamura, K., and Nakahata, T. (2003) Complete reconstitution of human lymphocytes from cord blood CD34 cells using the NOD/SCID/gammacnull mice model. *Blood* **102,** 873–880
26. Kambe, N., Hiramatsu, H., Shimonaka, M., Fujino, H., Nishikomori, R., Heike, T., Ito, M., Kobayashi, K., Ueyama, Y., Matsuyoshi, N., Miyachi, Y., and Nakahata, T. (2004) Development of both human connective tissue-type and mucosal-type mast cells in mice from hematopoietic stem cells with identical distribution pattern to human body. *Blood* **103,** 860–867
27. Tomita, M., Yamamoto, K., Kobashi, H., Ohmoto, M., and Tsuji, T. (1994) Immunohistochemical phenotyping of liver macrophages in normal and diseased human liver. *Hepatology* **20,** 317–325
28. Cramer, T., Schuppan, D., Bauer, M., Pfander, D., Neuhaus, P., and Herbst, H. (2004) Hepatocyte growth factor and c-Met expression in rat and human liver fibrosis. *Liver. Int.* **24,** 335–344
29. Ljubimova, J. Y., Petrovic, L. M., Wilson, S. E., Geller, S. A., and Demetriou, A. A. (1997) Expression of HGF, its receptor c-met, c-myc, and albumin in cirrhotic and neoplastic human liver tissue. *J. Histochem. Cytochem.* **45,** 79–87
30. Selzner, N., Selzner, M., Odermatt, B., Tian, Y., Van Rooijen, N., and Clavien, P. A. (2003) ICAM-1 triggers liver regeneration through leukocyte recruitment and Kupffer cell-dependent release of TNF-alpha/IL-6 in mice. *Gastroenterology* **124,** 692–700
31. Manz, M. G., Miyamoto, T., Akashi, K., and Weissman, I. L. (2002) Prospective isolation of human clonogenic common myeloid progenitors. *Proc. Natl. Acad. Sci. U. S. A.* **99,** 11872–11877
32. Wang, X., Montini, E., Al-Dhalimy, M., Lagasse, E., Finegold, M., and Grompe, M. (2002) Kinetics of liver repopulation after bone marrow transplantation. *Am. J. Pathol.* **161,** 565–574

Received for publication March 24, 2006.
Accepted for publication May 10, 2007.